Estuarine, Coastal and Shelf Science 218 (2019) 1–8

Contents lists available at ScienceDirect

Estuarine, Coastal and Shelf Science

journal homepage: www.elsevier.com/locate/ecss

Regulation of protist grazing on bacterioplankton by hydrological conditions in coastal waters

Xiangfu Li[a], Jie Xu[a,b,*], Zhen Shi[a], Dapeng Xu[c], Ruihuan Li[a], Qian Li[a], Hongbin Liu[d]

[a] State Key Laboratory of Tropical Oceanography, South China Sea Institute of Oceanology, Chinese Academy of Sciences, Guangzhou, 510301, China
[b] College of Earth Science, University of Chinese Academy of Sciences, Beijing, 100049, China
[c] State Key Laboratory of Marine Environmental Science, Institute of Marine Microbes and Ecosphere, College of Ocean and Earth Sciences, Xiamen University, Xiamen, 361102, China
[d] Division of Life Sciences, Hong Kong University of Science and Technology, Clear Water Bay, Kowloon, Hong Kong

ARTICLE INFO

Keywords:
Protist grazing
Bacterioplankton
Front
Deep chlorophyll maximum layer
Density gradient
The northern south China sea

ABSTRACT

A series of dilution experiments were conducted along an environmental gradient in coastal waters during April to September 2016, in order to examine the regulation of protist grazing on bacterioplankton by physical processes. Our results suggested that the density gradient in the frontal zone and the pycnocline played a significant role in regulating protist grazing on bacterioplankton in marine environments. The highest bacterial growth rate (1.33 d^{-1}) and grazing rate (1.05 d^{-1}) occurred in the frontal zone along the inshore-offshore transect and in the deep chlorophyll maximum (DCM) that always matched with the pycnocline in terms of the vertical profile in offshore waters. Spatial variability in bacterial growth rate and grazing rate was related to the presence of the density gradient in the front and the DCM. The density gradient aggregated phytoplankton and bacterial cells, enhancing their biomass. Meanwhile, high phytoplankton biomass provided more labile organic carbon to bacterioplankton in the front and the DCM, improving bacterial growth. Hence, the density gradient improved bacterial abundance, consequently enhancing the efficiency of protist grazing. Our findings implied that the density gradient improved bacterial carbon converted to high trophic levels and altered carbon flow in microbial food web in marine environments.

1. Introduction

Heterotrophic bacteria play an important role in carbon cycles by incorporating dissolved organic carbon (DOC) to produce new biomass and transforming DOC into inorganic carbon (Williams, 1981; Pomeroy et al., 1991; Fuhrman, 1992). Viruses and protists are two top-down regulators of bacterial mortality. Viruses transform bacterial biomass to DOC through viral shunt (Wilhelm and Suttle, 1999; Xu et al., 2013), while protists channel bacterial biomass to higher trophic levels through grazing (McManus and Fuhrman, 1988; Connell et al., 2017). Models and empirical observations show that viruses seem to significantly affect prokaryotic community diversity (Weinbauer and Rassoulzadegan, 2004; Cram et al., 2016) while protist grazing more likely regulates the abundance and biomass of bacteria (Baltar et al., 2016; Thingstad, 2000). Pernthaler (2005) suggests that effect of protist grazer on prokaryotes varies along the inshore-offshore gradient.

The ocean is highly structured horizontally and vertically due to the interaction of water masses, especially in coastal waters. Ocean structures (e.g. front, eddies and stratification) results in particle aggregation and retention, improving biological activity (Franks, 1992; Labat et al., 2009; Godø et al., 2012). A lot of attention has been paid to the effect of these physical features on phytoplankton biomass (Arin et al., 2013; d'Ovidio et al., 2010; McGillicuddy Jr, 2016), but little on bacterioplankton and zooplankton. A recent study shows that plankton patchiness is observed in the frontal region of West Spritsbergen Shelf (Trudnowska et al., 2016). However, little is known about how changes in physical features and environmental conditions affect microbial processes in marine environments. It is crucial to better understand the carbon cycling in oceans.

The South China Sea (SCS) with an area of 3.5×10^6 km^2, is located in the tropical to subtropical western North Pacific. The main basin of the northern SCS is characterized by oligotrophy (Xu et al., 2008). The northern SCS is influenced by the Pearl River discharge in summer, since the southwest monsoon and the Coriolis effect along the coast drive the offshore movement of the river plume (Watts, 1973; Yin, 2002). The Pearl River is the second largest river in China based on

* Corresponding author. State Key Laboratory of Tropical Oceanography, South China Sea Institute of Oceanology, Chinese Academy of Sciences, Guangzhou, 510301, China.
E-mail address: xujie@scsio.ac.cn (J. Xu).

https://doi.org/10.1016/j.ecss.2018.11.013
Received 13 March 2018; Received in revised form 29 October 2018; Accepted 15 November 2018
Available online 16 November 2018

freshwater discharge, and an annual average river discharge reaches $1.1 \times 10^4\ m^3\ s^{-1}$ (Zhao, 1990). Furthermore, around 80% of the river discharge occurs during the wet season (April–September), with a peak of the river discharge in July. The Pearl River discharge delivers huge amounts of nutrients to the adjacent coastal waters (Yin et al., 2001). Hence, there is a clear environmental gradient from inshore to offshore in the northern South China Sea during summer, which allowed us to examine our hypothesis that the density gradient induced by physical processes regulated protist grazing on bacterioplankton in marine environments.

2. Materials and methods

2.1. Study sites

Four cruises were conducted during a period from April to September 2016. Three stations (A1, A2 and A3) were visited in April 2016, five stations (B1, B2, B3, B4 and B5) in May 2016, six stations (C1, C2, C3, C4 C5 and C6) in June 2016 and five stations (D1, D2, D3, D4 and D5) in September 2016 in different oceanic regions: A1-A3, B1-B5, C1-C6 and D1-D2 in the inshore waters; D3-D5 in the offshore waters (Fig. 1). The edges of the inshore and offshore waters were defined as the 50 m contour line. Vertical profiles of temperature, salinity and fluorescence were measured with a CTD (Sea-bird) with a fluorescent probe. A salinity gradient of greater than $0.5\ km^{-1}$ is defined as the front in the study area. Water samples were taken at the surface (1 m below the sea surface) during a period from April to June 2016. However, water samples were collected at the surface (5–6 m below the sea surface), the deep chlorophyll maximum and the deep layer (33 m for D1, 37 m for D2, 190 m for D3, 300 m for D4 and D5) in September 2016. In addition, B3 and C1 were the same station, but visited in different months. That was the case for B4 and C2, as well as B5, C3 and D1.

2.2. Nutrients and chlorophyll a (Chl a)

Nutrient samples were filtered through glass fiber filters (GF/F) and then stored at −20 °C until analyzed. Nutrient concentrations were determined colorimetrically with a Seal AA3 autoanalyzer (Bran-Luebbe, GmbH). The concentrations of $NO_2 + NO_3$ and soluble PO_4 within the euphotic zone were measured according to the long-cell method (Li et al., 2008; Li and Hansell, 2008) with detection limits of 0.02 and 0.01 μM, respectively.

Water samples for Chl *a* were filtered onto glass fiber filters (GF/F) and stored at −20 °C until analysis. Chl *a* was extracted with 90% acetone and determined with a fluorometer (Turner Design) (Parsons et al., 1984).

2.3. Bacterial abundance

Water samples for bacterial abundance were collected in micro-centrifuge tubes, fixed with ice-cold glutaraldehyde (final concentration 0.5%) and subsequently stored in liquid nitrogen or −80 °C until analysis. Samples for counting bacteria were stained with 0.01% SYBR Green I in dark at room temperature for 45 min before they were determined by a flow cytometer (Becton-Dickinson Accuri TM C6) (Marie et al., 1997) and 1 μm beads were added.

2.4. Dilution experiments

A dilution experiment approach was used to estimate protist grazing rates (Tsai et al., 2013). Seawater was passed through a 20 μm mesh to remove meso- and microzooplankton and the filtrate was used as whole water (WW). The bacteria-free seawater was prepared by filtering seawater with a 0.2 μm cartridge. The whole water was diluted with 0.2 μm filtrate to produce 4 different dilution levels: 25%, 50%, 75% and 100% of WW. Samples were incubated in duplicate in 250 ml polycarbonate bottles in the dark for 24 h. Running seawater was used to maintain the surface *in situ* temperature. Samples for bacterial abundance were taken at the beginning and end of the incubations.

The net growth rate of bacteria was estimated based on bacterial abundance (N_0 and N_f) at the beginning (t_0) and the end of the experiment (t_f), according to the following equations (Landry and Hassett, 1982):

$$\mu = \ln(N_f/N_0)/(t_f - t_0)$$

The slope of the regression line in the plot of apparent growth rate versus dilution factor in the experiment was interpreted as protist grazing rate (g).

In this study, bacterial production (BP, μg C L^{-1} d^{-1}) and loss rate due to grazing (BG, μg C L^{-1} d^{-1}) were estimated according to the following equations described by Tsai et al. (2013):

$$BP = \mu \times B_0,$$

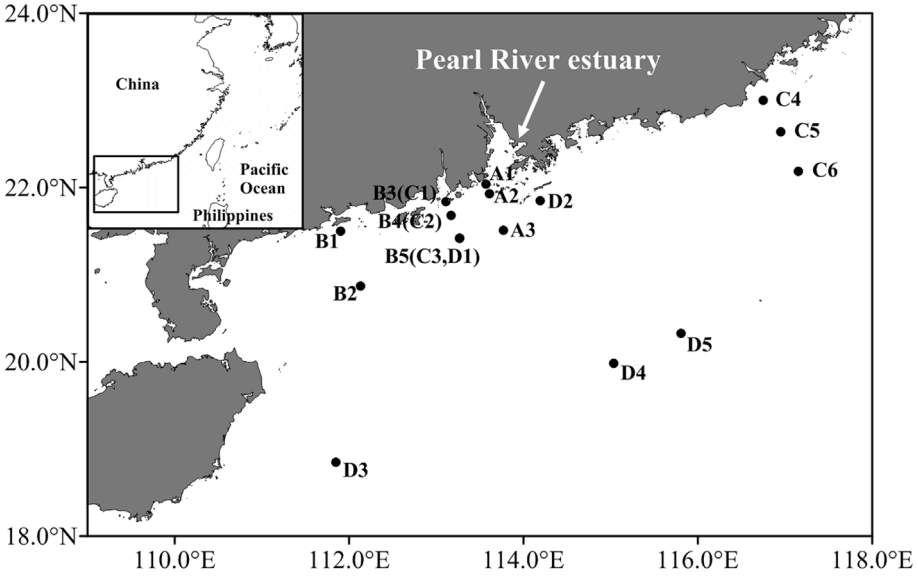

Fig. 1. The location of sampling stations in the northern South China Sea.

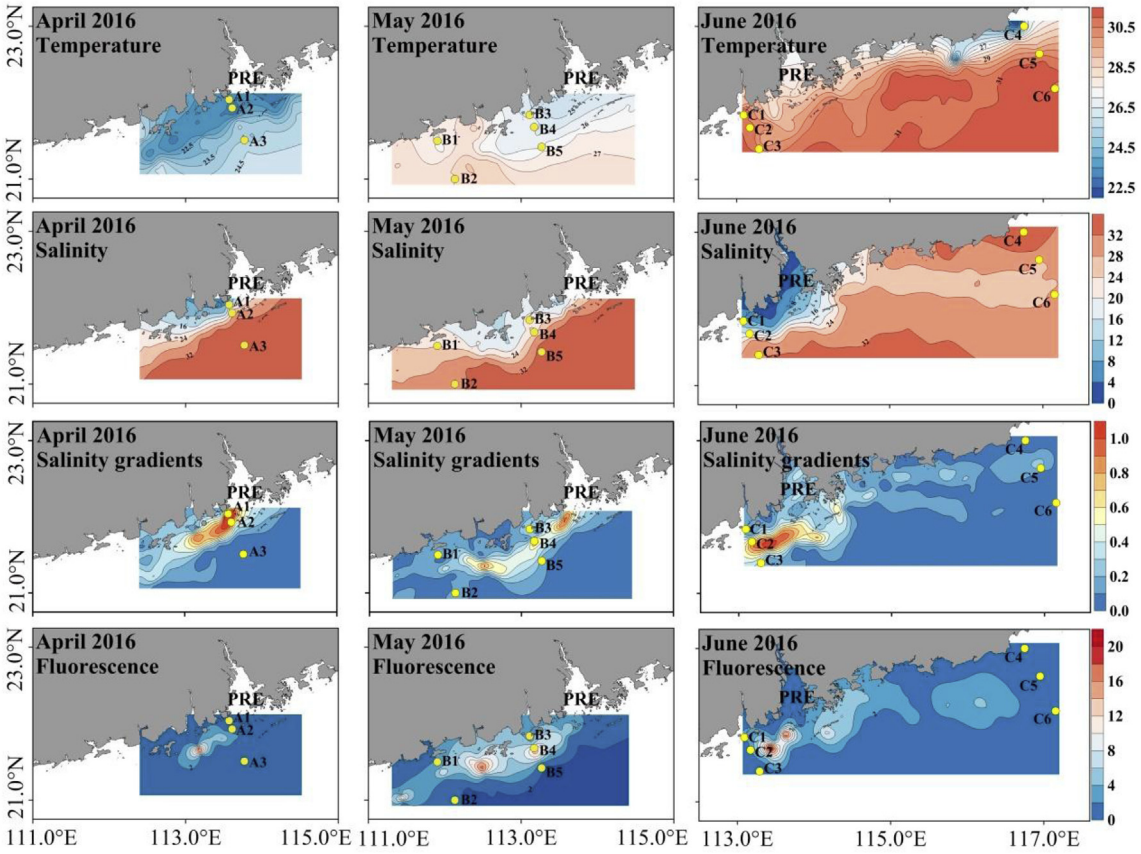

Fig. 2. The horizontal distribution of temperature, salinity, salinity gradient and fluorescence at the surface in the study area during the period from April to June 2016.

$BG = g \times B_0$,

Where μ is the dilution-based specific bacterial growth rate (y-intercept of the regression line), g is the dilution-based grazing rate, and B_0 is bacterial biomass (μg C L^{-1}) at the sampling time. Bacterial biomass is calculated with multiplying BA by bacterial cell quota (i.e. 20 fg C $cell^{-1}$) (Lee and Fuhrman, 1987).

2.5. Statistical analyses

The relationship between biological and environmental variables was analyzed using the SPSS program 17.0 (Pearson-test).

3. Results

3.1. Salinity and temperature

There was a great gradient in surface salinity and temperature from inshore to offshore during April to June 2016 (Fig. 2 and Table 1). At Station A1 near the Pearl River estuary, surface salinity was as low as 5.70. A front was formed in each cruise between the river plume and offshore shelf water, with high salinity (surface salinity > 32) water on the oceanic side of the front. In June 2016, the upwelling occurred at Station C4 with higher salinity and lower temperature than the surrounding waters (Fig. 2). In September 2016, surface salinity at two inshore stations (D1 and D2) was relatively low (28.4 and 32.1) compared to that (> 33.3) at offshore stations (D3-D5) (Fig. 3 and Table 1). Stratification occurred at all stations in september (see Fig. 3).

3.2. Nutrients and Chl a

During April to June 2016, DIN concentrations varied in a wide range from 108 μM at B3 to below the detection limit at offshore stations in three cruises. DIN decreased generally from inshore to offshore an increased from surface to the deep layer at offshore stations. However, PO_4 concentrations were relatively low and mostly lower than 0.30 μM, except for A1 where PO_4 was 0.91 μM (Table 1). Chl *a* concentration was the highest (6.62 μg L^{-1} at A2 and 8.04 μg L^{-1} at B4) in the front for each cruise, intermediate (0.88–4.53 μg L^{-1}) inside the front and lowest (0.39–1.07 μg L^{-1}) outside front. At the upwelling station (C4), Chl *a* concentration (1.06 μg L^{-1}) was comparable to that (1.07 μg L^{-1}) at C6 with the influence of the river plume (Table 1).

In September 2016, at offshore stations (D3, D4 and D5), nutrient and Chl *a* concentrations were very low. Nutrient concentrations were the lowest at the surface, (DIN < 0.1 μM, PO_4 < 0.1 μM), intermediate (DIN 0.10–1.71 μM, PO_4 0.14–0.25 μM) in the DCM layer and the highest (DIN > 10 μM, PO_4 > 1 μM) in the deep water (Table 1). Chl *a* concentrations were lower than 0.6 μg L^{-1} and it reached a peak in the deep chlorophyll maximum (Table 1). At inshore stations (D1 and D2), the concentrations of nutrients and Chl *a* were relatively high. DIN and PO_4 were up to 8.68 μM and 0.72 μM, respectively, and Chl *a* was up to 9.98 μg L^{-1} (Table 1).

3.3. Bacterial abundance, bacterial growth rate and grazing rate

Bacterial abundance exhibited spatial variability, with high (up to 3.80×10^9 cells L^{-1}) at inshore stations and low (< 3.93×10^8 cells L^{-1}) at offshore stations. During April to June 2016, bacterial abundance was higher in the front than outside the front (Fig. 4). In September 2016, bacterial abundance decreased with depth at all stations.

Bacterial growth rate lacked a clear spatial variability, ranging from 0.25 d^{-1} to 1.15 d^{-1} (Fig. 5). Protist grazing rates were generally higher at inshore station than those at the offshore stations. During

Table 1
Temperature, salinity, nutrients and Chl *a* concentrations at sampling stations.

Date	Stations	Depth(m)	Temperature(°C)	Salinity	DIN(μM)	PO3- 4(μM)	SiO2- 4(μM)	Chl *a* (μg L^{-1})
April 2016	A1	1	22.07	5.70	38.5	0.91	125	0.88
	A2	1	21.60	25.29	nd	0.12	nd	6.62
	A3	1	23.94	34.20	0.28	0.05	0.74	0.39
May 2016	B1	1	26.45	22.78	76.4	0.10	21.2	2.41
	B2	1	27.87	30.89	10.4	0.13	4.46	0.78
	B3	1	25.06	22.39	108	0.26	38.8	4.53
	B4	1	25.82	21.53	na	0.13	25.6	8.04
	B5	1	25.71	33.51	nd	0.07	0.35	0.82
June 2016	C1	1	31.45	8.30	na	na	na	na
	C2	1	30.87	15.83	na	na	na	na
	C3	1	30.98	30.93	3.29	0.10	0.57	1.06
	C4	1	26.25	33.56	1.73	0.03	14.4	1.07
	C5	1	30.35	28.05	1.66	0.05	0.92	0.81
	C6	1	31.31	28.04	3.39	0.06	0.63	1.06
September 2016	D1	6	28.43	28.37	8.68	0.09	2.16	9.98
	D1	33	23.26	34.59	4.21	0.46	13.2	0.65
	D2	5	28.75	32.14	0.08	0.10	2.02	0.48
	D2	17	25.78	33.62	2.64	0.07	8.39	6.73
	D2	37	23.19	34.50	6.31	0.72	22.4	0.95
	D3	5	29.87	33.98	0.06	na	1.60	0.33
	D3	50	24.58	34.59	0.10	0.14	2.92	0.52
	D3	190	15.49	34.57	13.2	1.08	14.7	0.01
	D4	5	29.71	33.67	0.07	0.08	2.07	0.05
	D4	65	23.77	34.65	1.71	0.25	4.15	0.45
	D4	300	11.70	34.40	17.3	1.58	28.2	0.01
	D5	5	29.66	33.30	0.06	0.08	2.06	0.11
	D5	80	23.21	34.66	0.69	0.21	3.79	0.27
	D5	300	11.17	34.39	22.60	1.77	37.2	0.01

Note: DIN = NO_3^- + NO_2^- + NH_4^+. na = not available. nd = undetectable.

April to June 2016, protist grazing rate reached a peak (0.96 d^{-1} at A2 in April, 1.05 d^{-1} at B4 in May, and 0.53 d^{-1} at C2 in June) in the frontal zone of each cruise (Fig. 5).

3.4. Bacterial production (BP) and bacterial carbon losses due to protist grazing

BP was generally higher at inshore stations than at offshore stations. In April and May 2016, the maximum (39.4 μg C L^{-1} d^{-1} at A2 and 35.9 μg C L^{-1} d^{-1} at B4) of BP was observed at the stations located in the frontal zone, while the minimum of BP occurred (3.34 μg C L^{-1} d^{-1} at A3, and 8.45 μg C L^{-1} d^{-1} at B5) outside the front (Fig. 6). In September, BP decreased from 20.8 μg C L^{-1} d^{-1} at inshore stations to as low as 0.72 μg C L^{-1} d^{-1} at offshore stations (Fig. 6).

Bacterial carbon losses induced by protist grazing (BG) varied in a wide range from 0.22 to 79 μg C L^{-1} d^{-1} (Fig. 6). During April to June 2016, in inshore waters, BG was the highest (up to 79 μg C L^{-1} d^{-1}) in the front. In offshore waters (e.g. D3, D4 and D5), BG (0.55–2.24 μg C L^{-1} d^{-1}) at the surface was similar to that (0.64–2.77 μg C L^{-1} d^{-1}) in the DCM, which was much higher than that (< 0.40 μg C L^{-1} d^{-1}) in deep water (Fig. 6).

The ratio of bacterial carbon losses to bacterial production varied from 221% to 10.2%, with the highest (221%) in the frontal zone and lowest (10.2%) in oligotrophic waters (Fig. 7).

4. Discussion

4.1. Variability in environmental conditions

The open ocean is typically oligotrophic in the South China Sea (Xu et al., 2008). In offshore waters (e.g. Stations D3, D4 and D5), DIN and PO_4 concentrations were < 0.1 μM and Chl *a* levels were < 1 μg L^{-1} in surface waters. Chl *a* concentration in the DCM layer was 1.5–9-fold higher than that at the surface. Bacterial abundance was low, with 3.24×10^8 to 3.93×10^8 cells L^{-1} at the surface, and decreased to 6.36×10^7 to 6.73×10^7 cells L^{-1} in the mesopelagic waters, which

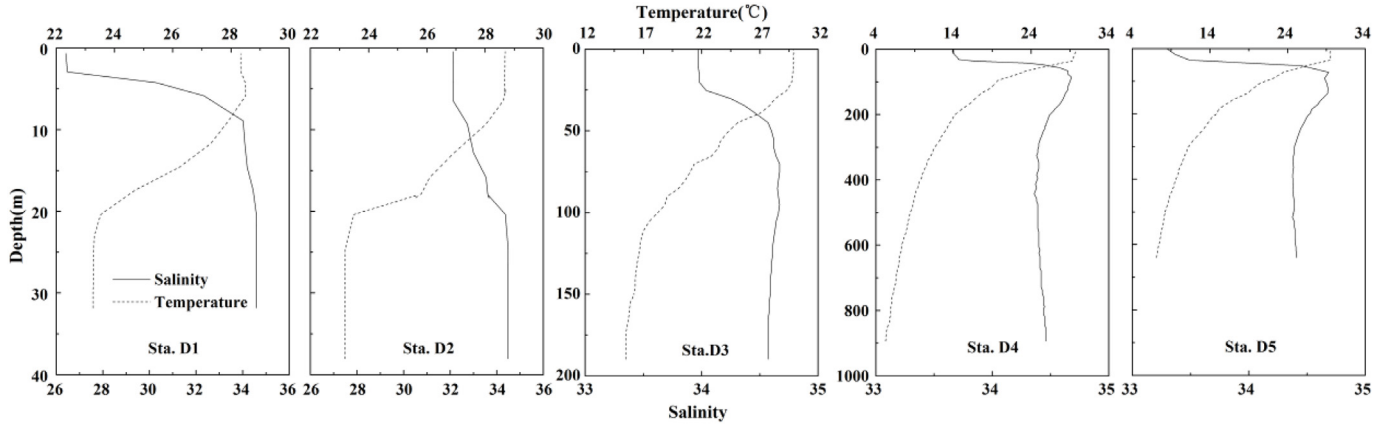

Fig. 3. The vertical profile of salinity and temperature at five stations in September 2016.

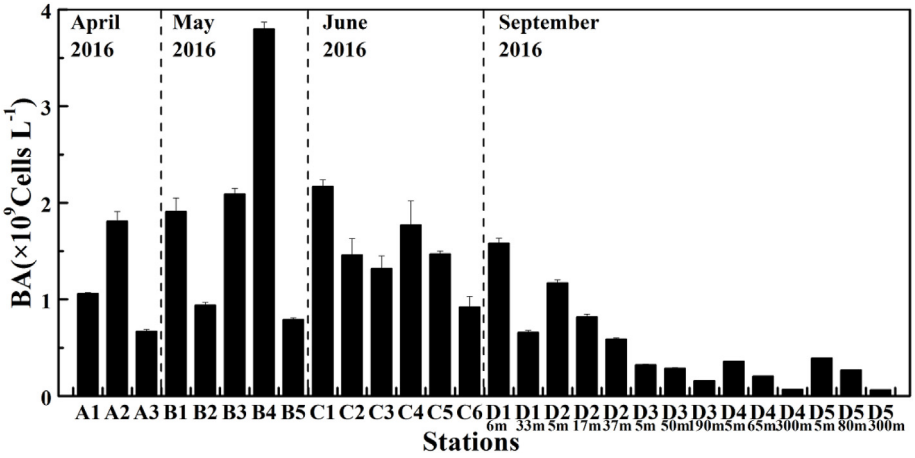

Fig. 4. Bacterial abundance at sampling stations. Vertical bars indicate ± 1 SD.

was comparable to that in other oceanic waters, such as the North Atlantic Ocean and NW Mediterranean Sea (Baltar et al., 2007; Gomes et al., 2015).

The Pearl River discharge delivers huge amounts of nutrients to coastal waters, leading to a large gradient in trophic conditions in the northern South China Sea (Xu et al., 2008). The river discharge alters seasonally due to a seasonal switch in monsoon winds. The freshwater discharge flowed out of the estuary to move westward and was confined to the nearshore area in April and May 2016 under the prevalence of the northeast monsoon. By contrast, the river plume moved eastward and extended to the shelf in the northern South China Sea in June 2016 when the southwest monsoon dominated. A hydrographic front was formed in the adjacent coastal waters due to the invasion of the freshwater, as shown by a clear gradient in salinity and temperature (Fig. 2). Surface salinity varied in a wide range from 5.70 to 34.6 across the front in inshore waters. The highest Chl *a* concentrations (up to 8.04 μg L^{-1}) always occurred in the frontal zone among three cruises during April to June 2016, accompanied by high bacterial abundance (up to 3.80 × 10^9 cells L^{-1}) and production (39.4 μg C L^{-1} d^{-1}). A significant correlation between Chl *a* concentration and bacterial abundance and production (Table 2) suggested that phytoplankton-derived DOC fueled bacterial growth. The coupling of phytoplankton biomass and bacterial production has been documented in other areas (Gasol et al., 1998; Gomes et al., 2015). Hence, nutrient enrichment induced by the river discharge stimulated phytoplankton growth, enhanced phytoplankton-derived DOM availability and subsequently promoted bacterial growth.

In our study, the sampling sites covered the eutrophic waters, front, oligotrophic waters and DCM. The dramatic difference in trophic conditions and hydrodynamic features in the study area allowed us to address regulation of protist grazing on bacterioplankton by physical processes and environmental conditions.

4.2. Regulation of protist grazing on bacterioplankton by physical features

Protist grazing on bacterioplankton varied spatially along the inshore to offshore transect. Grazing rates were generally high at inshore stations and low at offshore stations. However, the highest grazing rate occurred always in the frontal zone, instead of eutrophic nearshore stations (i.e. A1 and C1). In the frontal zone, grazing rates were even higher than bacterial growth rates, with the ratio of bacterial carbon losses to bacterial production being up to 221% and 130%at Stations B4 and C2, respectively (Figs. 5 and 7). Despite high grazing rates, the highest bacterial abundance still occurred in the frontal zone on the inshore-offshore transect. Hence, it was speculated that the maximum bacterial abundance in the frontal zone was the most likely due to the aggregation. A recent study has confirmed that plankton (phytoplankton, bacteria, small and medium zooplankton) and particles aggregate at density discontinuities, such as the horizontal density gradient on the hydrographic front, the vertical density gradient at the pycnocline (Trudnowska et al., 2016). The density gradient could act as a barrier to particle and plankton movement, which favored the maintenance of their position near preferred habitats (Trudnowska et al., 2016). On the other hand, high phytoplankton biomass at the density gradient (e.g. front and pycnocline) provided more labile phytoplankton-derived DOC to favor bacterial growth, as inferred by a

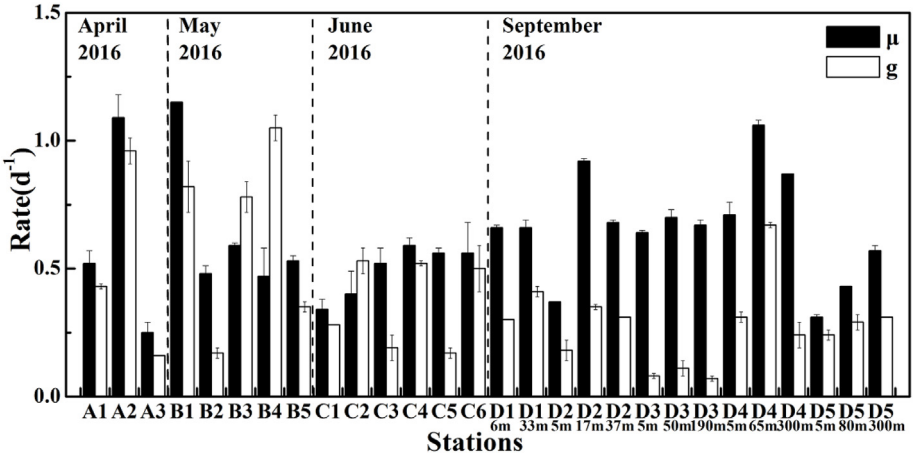

Fig. 5. Bacterial growth rate and protist grazing rate at sampling stations. Vertical bars indicate ± 1 SD.

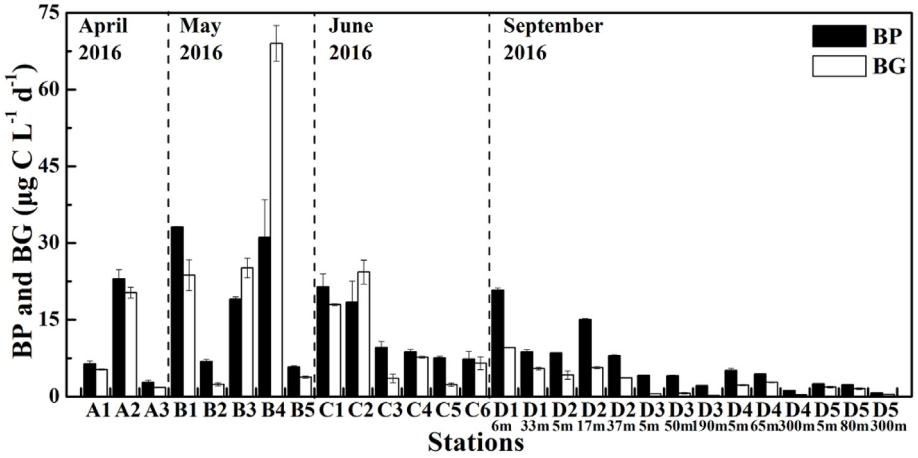

Fig. 6. Bacterial production (BP) and the carbon losses by protist grazing (BG) at sampling stations. Vertical bars indicate ± 1 SD.

significant correlation between Chl *a* and BP (Table 2). In the hydrographic front, high bacterial abundance was the result of mechanical aggregation of bacterial cells and high growth rates of bacterioplankton induced by high availability of phytoplankton-derived DOC. The enhanced bacterioplankton abundance improved the efficiency of protist predation, as indicated by a significant correlation between protist grazing rate with bacterial abundance and production. Our suggestion was in agreement with previous findings that the predation on prokaryotes increases with their abundance (Chiang et al., 2013; Sanders et al., 1992).

In offshore waters, bacterial growth rate and grazing rate were the highest in the DCM layer that often matched with the pycnocline, except for Station D5 where they reached a peak in deep waters. This scenario was similar to that in the hydrographic front. In contrast, in offshore waters, bacterial abundance was the highest at the surface, followed by that in the DCM layer, which was likely attributed to high grazing rate in the DCM layer. Similarly, Vaqué et al. (2017) found that higher protist abundance in the DCM layer than in the surface and the dominance of grazing in bacterial mortality over viral infection. In our study, high grazing rates observed in the hydrographic front and the DCM layer were attributed to high bacterial abundance in the density gradient.

Bacterial carbon converted to the higher trophic levels of food webs ranged from 0.22 to 79 μg C L^{-1} d^{-1}, comparable to the values observed in Taiwan coastal region (Tsai et al., 2013). In inshore waters, bacterial carbon ingested by protists reached a maximum (79 μg C L^{-1} d^{-1}) in eutrophic waters or the frontal zone in the inshore waters owing to high bacterial abundance and grazing rate. In the frontal zone (i.e. B4 and C2), bacterial carbon ingested by protists (79 μg C L^{-1} d^{-1} at B4 and 15 μg C L^{-1} d^{-1} at C2) surpassed bacterial production (35 μg C L^{-1} d^{-1} at B4 and 11 μg C L^{-1} d^{-1} at C2) (Fig. 6). Compared to those at eutrophic stations (e.g. A1, B3 and C1) and at stations (e.g. A3, B5 and C3) outside the front along the inshore-offshore transect, bacterial carbon losses due to protist grazing in the front were 1.3–3.8 folds and 3.0–16.4 folds higher, respectively. Hence, the density gradient (e.g. front and pycnocline) in the water column in marine environments promoted the carbon transfer to the high trophic levels in microbial

Table 2
The correlation between variables at all sampling stations.

	BA	μ	g	g: μ	BP	BG
Salinity	−0.58**		−0.38*	−0.53**	−0.40**	−0.40*
Temp.		−0.54**				
DIN	0.59**		0.67**	0.58**	0.65**	0.83**
PO3- 4						
SiO2- 4						
Chl *a*	0.68**		0.56**	0.48*	0.70**	0.63**
BA			0.66**	0.76**	0.83**	0.88**
μ			0.41*		0.39*	
g				0.79**	0.78**	0.84**
g: μ					0.54**	0.85**
BP						0.81**
BG						

Note: * denotes significant correlation at the 0.05 level, ** denotes significant correlation at the 0.01 level. The numbers denote the correlation coefficients (r).

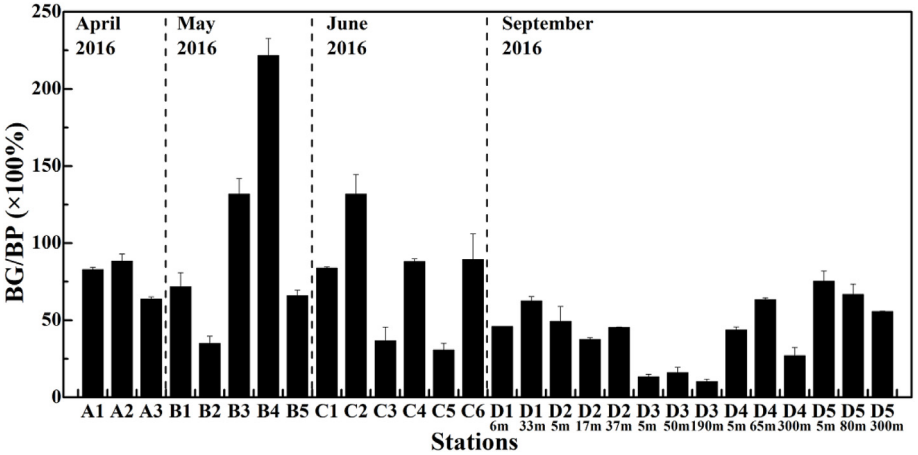

Fig. 7. The ratio of bacterial carbon losses by protist grazing (BG) to bacterial production (BP). Vertical bars indicate ± 1 SD.

food webs by aggregating bacterial cells and improving grazing efficiency. Our findings implied that physical processes played an important role in regulating the carbon transfer in microbial food web in marine environments, which was in agreement with previous reports that physical features (e.g. front or eddies) create attractive feeding habitats for higher trophic levels (Bakun, 2006; Godø et al., 2012).

4.3. Consideration on the dilution experiments

In water samples, phytoplankton growth would increase phytoplankton-derived DOC supply and further enhance bacterial abundance, which might lead to overestimate of grazing rates, since protist grazing rates increase with bacterial abundance (Sanders et al., 1992). The dilution experiments are usually conducted in dark for the determination of grazing rate on bacterioplankton, in order to suppress the phytoplankton growth in water samples and simplify the interaction of protist and bacterioplantkon. Our dilution experiments were incubated for a short time (24 h) to mitigate artificial effects on the plankton community. In addition, different groups of zooplankton generally graze preys in different sizes. In the Pearl River estuary and its adjacent coastal waters, phytoplankton are dominated by diatoms (Xu et al., 2009; Qiu et al., 2010), who is in size much larger than bacterioplankton. In water samples, bacterivorous predators should hardly feed on large phytoplankton, such as diatoms.

5. Summary

Physical processes played a significant role in regulating protist grazing on bacterioplankton in marine environments. The density gradient that occurred in the frontal zone or the pycnocline aggregated plankton. Meanwhile, enhanced phytoplankton biomass increased labile phytoplankton-derived DOC availability to fuel bacterioplankton growth in the frontal zone and the pycnocline. As a result, high bacterial abundance increased grazing efficiency, leading to high grazing rate. Hence, the presence of the density gradient promoted the transfer of bacterial carbon to the high tropical levels. Our findings improved our understanding of dynamics of the carbon flow in microbial food web across marine environments.

Acknowledgements

Financial support for this research was granted by the project of Qingdao National Laboratory for Marine Science and Technology (No. QNLM2016ORP0305), National Natural Science Foundation of China (No. 41476137, 41676075), the Project of State Key Laboratory of Tropical Oceanography, (LTOZZ1705), Hundred Talent Program of Chinese Academy of Sciences,. We thank Prof Dongxiao Wang for providing the data of temperature, salinity and fluorescence.

Appendix A. Supplementary data

Supplementary data related to this article can be found at https://doi.org/10.1016/j.ecss.2018.11.013.

References

d'Ovidio, F., De Monte, S., Alvian, S., Dandonneau, Y., Levy, M., 2010. Fluid dynamical niches of phytoplankton types. Proc. Natl. Acad. Sci. U.S.A. 107, 18366–18370.
Fuhrman, J.A., 1992. Bacterioplankton roles in cycling of organic matter: the microbial food web. In: Woodhead, P.G.F. (Ed.), Primary Productivity and Biogeochemical Cycles in the Sea. Plenum Press, NewYork, pp. 361–383.
Arin, L., Guillén, J., Segura-Noguera, M., Estrada, M., 2013. Open sea hydrographic forcing of nutrient and phytoplankton dynamics in a mediterranean coastal ecosystem. Estuar. Coast Shelf Sci. 133, 116–128.
Bakun, A., 2006. Fronts and eddies as key structures in the habitat of marine fish larvae: opportunity, adaptive response and competitive advantage. Sci. Mar. 70S2, 105–122.
Baltar, F., Arístegui, J., Gasol, J.M., Hernández-León, S., Herndl, G.J., 2007. Strong coast–ocean and surface–depth gradients in prokaryotic assemblage structure and activity in a coastal transition zone region. Aquat. Microb. Ecol. 50, 63–74.
Baltar, F., Palovaara, J., Unrein, F., Catala, P., Horňák, K., Šimek, K., Vaqué, D., Massana, R., Gasol, J.M., Pinhassi, J., 2016. Marine bacterial community structure resilience to changes in protist predation under phytoplankton bloom conditions. ISME J. 10, 568–581.
Chiang, K.P., Tsai, A.Y., Tsai, P.J., Gong, G.C., Tsai, S.F., 2013. Coupling of the spatial dynamic of picoplankton and nanoflagellate grazing pressure and carbon flow of the microbial food web in the subtropical pelagic continental shelf ecosystem. Biogeosci. Discuss. 10, 233–263.
Connell, P.E., Campbell, V., Gellene, A.G., Hu, S.K., Carona, D.A., 2017. Planktonic food web structure at a coastal time-series site: II.Spatiotemporal variability of microbial trophic activities. Deep-Sea Res. I 121, 210–223.
Cram, J.A., Parada, A.E., Furhman, J.A., 2016. Dilution reveals how viral lysis and grazing shape microbial communities. Limnol. Oceanogr. 61, 889–905.
Franks, P.J.S., 1992. Sink or swim: accumulation of biomass at fronts. Mar. Ecol. Prog. Ser. 82, 1–12.
Gasol, J.M., Doval, M.D., Pinhassi, J., Calderón-Paz, J.I., Guixa-Boixareu, N., Vaqué, D., Pedrós-Aliós, D., 1998. Diel variations in bacterial heterotrophic activity and in the northwestern Mediterranean Sea. Mar. Ecol. Prog. Ser. 164, 107–124.
Godø, O.R., Samuelsen, A., Macaulay, G.J., Patel, R., Hjøllo, S.S., Horne, J., Kaartvedt, S., Johannessen, J.A., 2012. Mesoscale eddies are oases for higher trophic marine life. PloS One 7, e30161.
Gomes, A., Gasol, J.M., Estrada, M., Franco-Vidal, L., Díaz-Pérez, L., Ferrera, I., Morán, X.A.G., 2015. Heterotrophic bacterial responses to the winter–spring phytoplankton bloom in open waters of the NW Mediterranean. Deep-Sea Res. I 96, 59–68.
Labat, J.P., Gasparini, S., Mousseau, L., Prieur, L., Boutoute, M., Mayzaud, P., 2009. Mesoscale distribution of zooplankton biomass in the northeast Atlantic Ocean determined with an optical plankton counter: relationships with environmental structures. Deep-Sea Res. I 56, 1742–1756.
Landry, M.R., Hassett, R.P., 1982. Estimating the grazing impact of marine microzooplankton. Mar. Biol. 67, 283–288.
Lee, S., Fuhrman, J.A., 1987. Relationships between biovolume and biomass of naturally derived marine bacterioplankton. Appl. Environ. Microbiol. 53, 1298–1303.
Li, Q.P., Hansell, D.A., 2008. Nutrient distributions in baroclinic eddies of the oligotrophic North Atlantic and inferred impacts on biology. Deep Sea Res. Part II 55 (10), 1291–1299.
Li, Q.P., Hansell, D.A., Zhang, J.Z., 2008. Underway monitoring of nanomolar nitrate plus nitrite and phosphate in oligotrophic seawater. Limnol Oceanogr. Methods 6, 319–326.
Marie, D., Partensky, F., Jacquet, S., Vaulot, D., 1997. Enumeration and cell cycle analysis of natural populations of marine picoplankton by flow cytometry using the nucleic acid stain SYBR Green I. Appl. Environ. Microbiol. 63, 186–193.
McGillicuddy Jr., D.J., 2016. Mechanisms of physical-biological-biogeochemical interaction at the oceanic mesoscale. Annu. Rev. Marine. Sci. 8, 125.
McManus, G.B., Fuhrman, J.A., 1988. Control of marine bacterioplankton populations: measurement and significance of grazing. Hydrobiologia 159, 51–62.
Parsons, T.R., Maita, Y., Lalli, C.M., 1984. A Manual of Chemical and Biological Methods for Seawater Analysis. Oxford Press, Pergamum.
Pernthaler, J., 2005. Predation on prokaryotes in the water column and its ecological implications. Nat. Rev. Microbiol. 3, 537–546.
Pomeroy, L.R., Wiebe, W.J., Deibel, D., Thompson, J.R., Rowe, G.T., Pakulski, J.D., 1991. Bacterial responses to temperature and substrate concentration during the Newfoundland spring bloom. Mar. Ecol. Prog. Ser. 75, 143–159.
Qiu, D.J., Huang, L.M., Zhang, J.L., Lin, S.J., 2010. Phytoplankton dynamics in and near the highly eutrophic Pearl River estuary, south China sea. Continent. Shelf Res. 30, 177–186.
Sanders, R.W., Caron, D.A., Berninger, U.G., 1992. Relationships between bacteria and heterotrophic nanoplankton in marine and fresh waters: an inter-ecosystem comparison. Mar. Ecol. Prog. Ser. 1–14 1992.
Thingstad, T.F., 2000. Elements of a theory for the mechanisms controlling abundance, diversity and biogeochemical role of lytic bacterial viruses in aquatic systems. Limnol. Oceanogr. 45, 1320–1328.
Trudnowska, E., Gluchowska, M., Beszcaynska-Möller, A., Blachowiak-Samolyk, K., Kwasniewski, S., 2016. Plankton patchiness in the Polar front region of the west Spitsbergen Shelf. Mar. Ecol. Prog. Ser. 560, 1–18.
Tsai, A.Y., Gong, G.C., Hung, J., 2013. Seasonal variations of virus- and protist-mediated mortality of heterotrophic bacteria in the coastal ecosystem of subtropical western Pacific. Biogeosciences 10, 3055–3065.
Vaqué, D., Boras, J.A., Torrent-Llagostera, F., Agusti, S., Arrieta, J.M., Lara, E., Castillo, Y.M., Duarte, C.M., Sala, M.M., 2017. Viruses and protists induced-mortality of prokaryotes around the antarctic peninsula during the austral summer. Front. Microbiol. 8, 241.
Watts, J.C.D., 1973. Further observation on the hydrology of the Hong Kong territorial waters. Hong Kong Fish. Bull 3, 9–35.
Weinbauer, M.G., Rassoulzadegan, F., 2004. Are viruses driving microbial diversification and diversity? Environ. Microbiol. 6, 1–11.
Wilhelm, S.W., Suttle, C.A., 1999. Viruses and nutrient cycles in the sea. Bioscience 49, 781–788.
Williams, P.J.L., 1981. Microbial contribution to overall marine plankton metabolism: direct measurement of respiration. Oceanol. Acta 4, 359–364.
Xu, J., Yin, K.D., He, L., Yuan, X.C., Ho, A.Y.T., Harrison, P.J., 2008. Phosphorus limitation in the northern South China Sea during late summer: influence of the Pearl River. Deep-Sea Res. I 55, 1330–1342.
Xu, J., Ho, A.Y.T., Yin, K.D., Anderson, D.M., Lee, J.H.W., Harrison, P.J., 2009. Nutrient limitation in Hong Kong waters inferred from comparison of bioassays and nutrient ratios, turnover times. Mar. Ecol. Prog. Ser. 388, 81–97.

Xu, J., Jing, H.M., Sun, M.M., Harrison, P.J., Liu, H.B., 2013. Regulation of bacterial metabolic activity by dissolved organic carbon and viruses. J. Geophys. Res. 118, 1573–1583.
Yin, K.D., 2002. Monsoonal influence on seasonal variations in nutrients and phytoplankton biomass in coastal waters of Hong Kong in the vicinity of the Pearl River estuary. Mar. Ecol. Prog. Ser. 245, 111–122.
Yin, K.D., Qian, P.Y., Wu, M.C.S., Chen, J.C., Huang, L., Song, X., Jian, W.J., 2001. Shift from P to N limitation of phytoplankton biomass across the Pearl River Estuarine plume during summer. Mar. Ecol. Prog. Ser. 221, 17–28.
Zhao, H., 1990. Evolution of the Pearl River Estuary. Ocean Press, Beijing (in Chinese).